Dyes and Pigments 188 (2021) 109173

Contents lists available at ScienceDirect

Dyes and Pigments

journal homepage: http://www.elsevier.com/locate/dyepig

pKa modulation of rhodamine alkylamides by hydrogen-bond and application in bio-imaging

Lei Min [a], Xintong Li [a], Weiliang Zhang [a], Xinfu Zhang [b], Ying Zhang [a,**], Haibo Yu [a,b,*], Yi Xiao [b]

[a] School of Environment, Liaoning University, Shenyang, 110036, China
[b] State Key Laboratory of Fine Chemicals, Dalian University of Technology, Dalian, 116024, China

ARTICLE INFO

Keywords:
Rhodamine alkylamides
Hydrogen bond
pKa tuning
Fluorescent probe
Lysosome imaging

ABSTRACT

To confirm the pKa regulation by hydrogen bond, a series of rhodamine alkylamides were developed, and their pKa values were measured in aqueous solution. For Rh-APD, intramolecular hydrogen bond derived from hydroxyl of 2-amino-1,3-propanediol between carbonyl of spirolactam was favorable to the increase of pKa values (pKa 5.7). Gaussian stimulation demonstrated a moderate intramolecular hydrogen bond in Rh-APD at DFT/B3LYP/6–31 G(d) level. Except for pH, neither protic/aprotic solvents nor metal ions induced ring-opening transformation of Rh-APD. Bio-imaging showed that Rh-APD could specifically accumulate in lysosomes and evaluate lysosomal pH fluctuation in living MCF-7 cells. Moreover, Rh-APD also can indicate the acidity of gut and ovary of Daphnia magna. Rh-APD would be a potential reagent for water-quality monitoring with the help of its pH indication in living cells and water fleas.

1. Introduction

Rhodamine spirolactam has captured great attention for its ring-switching character, which is applied in many fields such as fluorescent sensors[1,2], printing and dyeing[3,4], thermo-sensitive materials [5,6], optoelectronic devices[7,8], and super-resolution imaging[9,10], etc. The switching transformation of rhodmaine spirolactam between colorless spirolactam and fluorescent zwitterions is highly sensitive to pH of solvents. Then it has been used to design a lot of pH fluorescent probes based on rhodamine spirolactam[11–13]. Various primary amines have been utilized to develop pH probes with different pKa value and applied in acidic or neutral monitoring[14–25]. The pKa value of these probes is an important parameter for the range of pH response and its accumulation in living cells. Generally, primary amines, such as hydrazine derivatives [14–17], ethanediamine derivatives [18–22] amino acid analogs [23,24], are widely used in the design of rhodamine spirolactams for pH indicators. The vast majority of primary amines are flexible aliphatic chain in the structure of rhodamine spirolactams, whose pKa values are usually in a broad range from 3.0 to 5.2[14–24]. Steric hindrance and substitute effect have been proposed to modulate the pKa values of rhodamine spirolactams with large steric hindrance, such as aniline derivatives[25–27]. Nevertheless, there is little method to modulate the pKa of rhodamine alkylamides bearing aliphatic chain.

The freewheeling regulation between ring-opening and closing form of spirolactam is the goal of our pursuit[28–30]. Except for steric hindrance and substitute effect, positive charge from quaternary ammonium salt has been proofed to be an effective factor to water solubility and pH responses of rhodamine spirolactam[29,31]. In addition, with the aid of steric hindrance, we also have designed a rhodamine pH probe (Rh-Met) bearing methionine group with a neutral pKa 6.8, which can localize in mitochondria and droplet of living cells[30]. The neutral pKa of Rh-Met has been attributed to the steric hindrance and hydrogen bond (Scheme 1a). Considering flexible alkyl chain usually possesses small steric hindrance, hydrogen bond as the main factor would be beneficial for the neutral pKa. To further confirm the pKa regulation by hydrogen bond, herein, a series of flexible alkyl chains were introduced into rhodamine spirolactams, and the pKa values were measured in aqueous solution. Primary amines such as 2-amino-1,3-propanediol, ethanolamine, 3-pentanamine and the acetylation of amino-1,3-propanediol were used to develop a series of rhodamine alkylamides (Scheme 1). We anticipate that intramolecular hydrogen bond between the hydrogen in hydroxyl of amino-1,3-propanediol and oxygen in carbonyl of spirolactam would be conducive to the ring-opening reaction and stabilization of the zwitterions form, resulting a larger pKa value of rhodamine

* Corresponding author. School of Environment, Liaoning University, Shenyang, 110036, China.
** Corresponding author. School of Environment, Liaoning University, Shenyang, 110036, China.
E-mail addresses: yingying0809@126.com (Y. Zhang), yuhaibo@lnu.edu.cn (H. Yu).

https://doi.org/10.1016/j.dyepig.2021.109173
Received 3 January 2021; Received in revised form 21 January 2021; Accepted 21 January 2021
Available online 27 January 2021
0143-7208/

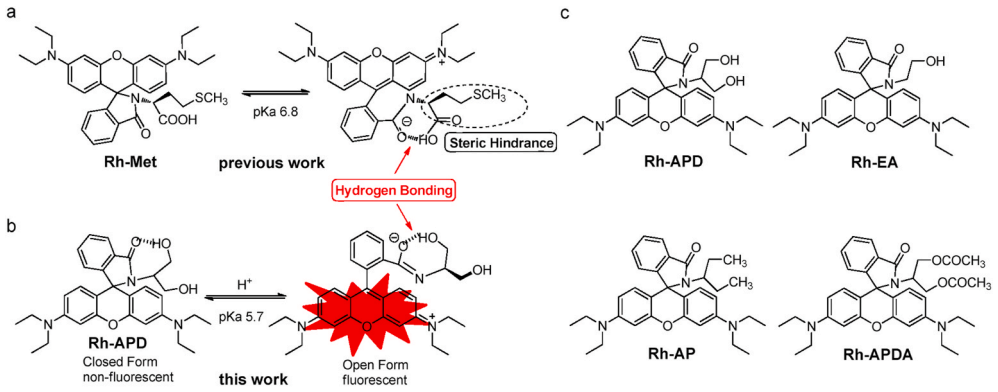

Scheme 1. Protonation procedure of (a) Rh-Met and (b) Rh-APD. (c) The structures of Rh-APD, Rh-EA, Rh-AP and Rh-APDA.

alkylamides (Scheme 1b). C. P. Pradeep et al. has reported a rhodamine alkylamides containing tris(hydroxymethyl)aminomethane, which can be always in a ring-opening form in protic solvents owing to the hydrogen-bonding stabilization[32]. Different from tris(hydroxymethyl)- aminomethane-rhodamine spirolactam, the ring switch of Rh-APD was expect to be modulated by pH, but not by protic or aprotic solvents.

2. Experimental

2.1. Synthesis of Rh-APD

Rhodamine B acid chloride (RhB–Cl) was obtained, according to the procedure previously reported[33]. RhB–Cl was used without further purification. 2-amino-1,3-propanediol (94.8 mg, 1.04 mmol) was dissolved in 2 mL C_2H_5OH solution containing 3 mL NEt_3 and 3 mL CH_3CN. The mixtures were added dropwise into the solution above of crude acid chloride in 30 mL CH_3CN. After stirring overnight at room temperature, the solvent was removed by rotavapor. The crude product was purified through silica gel column chromatography with a mixture of dichloromethane and methanol (35:1, v/v) as eluent. Rh-APD was obtained as a pink powder (228.5 mg, Yield 43%). HRMS $[M+H]^+$ $C_{31}H_{38}N_3O_4$ Calc. 516.2862 Found 516.2852, ^{1}H NMR (500 MHz, DMSO) δ 7.76–7.74 (m, 1H), 7.52–7.48 (p, J = 6.3 Hz, 2H), 6.99–6.97 (m, 1H), 6.39–6.34 (m, 6H), 4.52 (dd, J = 6.3, 4.9 Hz, 2H), 3.67–3.62 (m, 2H), 3.34–3.30 (m, 8H), 3.00 (m, J = 11.5, 6.1 Hz, 1H), 1.09 (t, J = 7.0 Hz, 12H). ^{13}C NMR (125 MHz, DMSO) δ 167.8, 153.3, 152.8, 148.4, 132.8, 130.9, 129.2, 128.3, 123.7, 122.2, 107.9, 104.3, 97.0, 65.6, 59.3, 57.1, 54.9, 43.6, 12.4.

2.2. pH titration

pH titration was carried out according to the method we reported previously[34]. In pH titration, the concentration of Rh-APD and its contrasting compounds was 2×10^{-5} M in C_2H_5OH/H_2O (v:v 1:1). Conc. HCl and NaOH were used during the pH titration. Meanwhile, the absorption and emission spectra was recorded in UV spectrophotometer and spectrofluorophotometer, respectively.

2.3. Cell and Daphnia magna culture

The procedure of MCF-7 cell culture can refer to that reported previously[35]. Parthenogenetic Daphnia magna was supplied by Shenyang Chemical Research Institute co. LTD. Daphnia magna was cultured in chlorine-free tap water (pH 7.8 ± 0.2) at room temperature (20 ± 2 °C) under daylight fluorescent lamps with the photoperiod 14/10 h (light/dark). The water was renewed every three days.

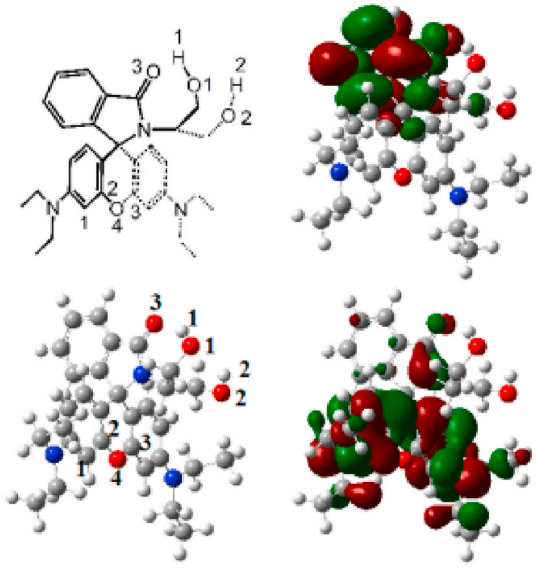

Fig. 1. The geometry of Rh-APD optimized by Gaussian (DFT/B3LYP/6–31 G(d)).

2.4. Fluorescence imaging of MCF-7 cells and Daphnia magna

MCF-7 cells in exponential phase of growth were stained with Rh-APD (5 μM) in an atmosphere of 5% CO_2 and 95% air at 37 °C for 10 min. After cells were washed three times with PBS, 5 μM DND-26 in 2 mL RPMI 1640 was added and cultured for 10 min. And then these cells were washed three times with PBS. Finally, added 1 mL RPMI 1640 culture medium and observed under confocal microscopy (IX81). Green Channel was excited at 488 nm laser and the BF was in the range from 500 nm to 520 nm. In Red Channel, the excitation wavelength was 559 nm and the emission signal was collected in the range from 575 nm to 655 nm. During co-localization imaging, the parameters of HV (sensitivity of detector) remain constant. Daphnia magna was taken in Rh-APD (5 μM) water solution contain 0.1% DMSO for 5 min. Daphnia magna was washed three times with chlorine-free tap water. Fluorescent imaging of Daphnia magna stained with Rh-APD was obtained from fluorescence microscope (BX-51).

3. Results and discussion

3.1. Geometry optimization

The optimized geometry of Rh-APD was simulated by Gaussian software at DFT/B3LYP/6–31 G(d) level. Similar to common

Table 1
The hydrogen-bond parameters of Rh-APD.

parameters	Rh-APD		Hydrogen bond model[36]		
	O1–H1···O3	O2–H2···O1	Strong	Moderate	Weak
A-H···B interaction	electrostatic	electrostatic	Mostly covalent	Mostly electrostatic	electrostatic
Bond lengths	O1–H1<H1–O3	O2–H2<H2–O1	A-H ≈ H···B	A-H < H···B	A-H ≪ H···B
H···B(Å)	1.850	2.106	~1.2–1.5	~1.5–2.2	2.2–3.2
A···B(Å)	2.732	2.814	2.2–2.5	2.5–3.2	3.2–4.0
Bond angle (°)[a]	146.4	127.3	175–180	130–180	90–150
δ_H (ppm)[b]	δ_{H1}5.75	δ_{H2}~3.3	14–22	<14	<14

[a] Bond angle of hydrogen bond, ∠AHB.
[b] Chemical shift of hydrogen in hydroxyl group, ppm.

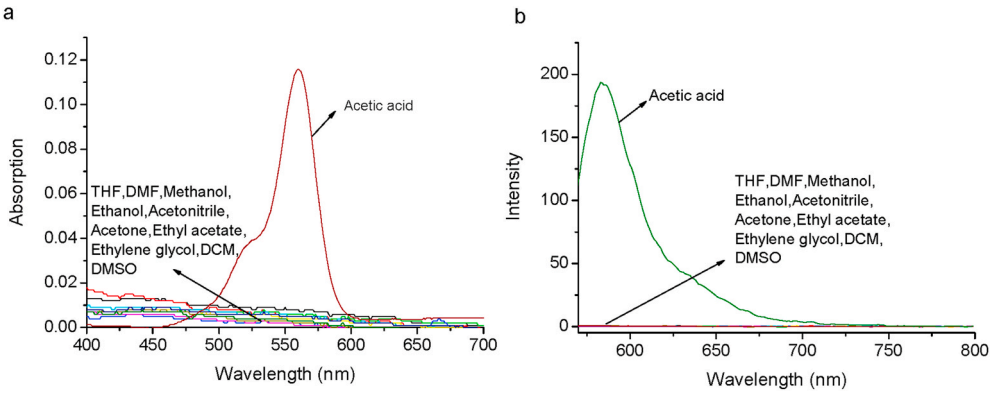

Fig. 2. Absorption (a) and emission (b) spectra of Rh-APD in protic, aprotic solvents and acetic acid (contain 50% C_2H_5OH v:v).

spirolactam, the five-member lactam in spatial structure was planar for Rh-APD. The dihedral angle of nonplanar xanthene ring (C1–C2–O4–C3) was 175.6° in accordance with common rhodamine spirolactam. However, it can be identified a moderate intramolecular hydrogen-bond from bond parameters measured in optimized geometry of Rh-APD (Fig. 1). The bond length of O1–H1 was 0.991 Å, which was a bit longer than that of O2–H2 (0.985 Å). Compared with hydrogen atom H2 in hydroxyl group, hydrogen atom H1 was close to oxygen atom O3 of amide in Rh-APD. The spatial distance of H1–O3 and O1–O3 was 1.850 Å and 2.732 Å, which were in their respective scope of moderate hydrogen bond (Table 1). Moreover, the distance of H1–O3 (1.850 Å) was shorter than that of O3–H2 (4.101 Å), but longer than that of O1–H1 (0.991 Å). The bond angle of O1–H1–O3 (146.4°) signalled that the intramolecular hydrogen bond in Rh-APD was mostly electrostatic interaction. Different from the strength of H1–O3 hydrogen bond, the H2–O1 interaction was much smaller according to hydrogen bond model reported by Jeffrey[36]. Finally, relatively large chemical shift of δ_H1 (5.75 ppm) provided further evidence that there was a moderate intramolecular hydrogen bond in Rh-APD. In addition, the electron distribution of HOMO and LUMO of Rh-APD was mainly delocalized on xanthene ring and five-member lactam, respectively.

3.2. Solvent effect of Rh-APD

Given the moderate hydrogen bond interaction, we anticipated that 2-amino-1,3-propanediol bearing two hydroxyl groups in Rh-APD would diminish the trend toward open-state transformation induced by protic solvent. Then, absorption and emission spectra of Rh-APD were respectively investigated in protic (glycol, methanol, ethanol) and aprotic solvents (THF, DCM, acetonitrile, acetone, ethyl acetate, DMF and DMSO). Either in methanol, ethanol or glycol, the absorption and emission peak was not observed in its spectra (Fig. 2). After acetic acid was added into Rh-APD solution of ethanol, a bright red color of Rh-APD solution appeared and the maximum of absorption peaked at 560 nm (Fig. 2a). Meanwhile, a strong fluorescent emission at 585 nm was observed upon irradiation with 560 nm light (Fig. 2b). These results

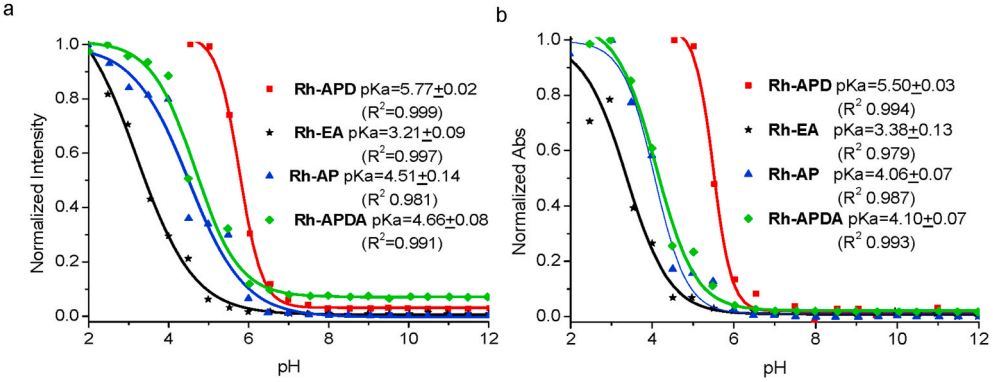

Fig. 3. Normalized emission (a) and absorption (b) of Rh-APD, Rh-EA, Rh-AP and Rh-APDA at maximum vs pH values in C_2H_5OH/H_2O solutions (v:v 1:1).

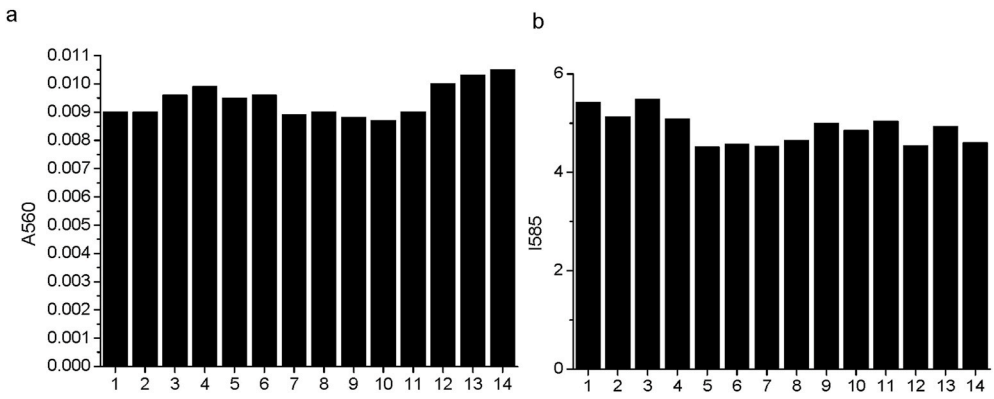

Fig. 4. (a) Absorption intensity at 560 nm and (b) emission intensity at 585 nm of Rh-APD in C_2H_5OH/tris-HCl buffer (1:1, v:v, pH 7.4) in the absence and presence of metal ions. 1 Blank, 2 Al^{3+}, 3 K^+, 4 Hg^{2+}, 5 Cr^{3+}, 6 Mn^{2+}, 7 Ca^{2+}, 8 Na^+, 9 Cd^{2+}, 10 Zn^{2+}, 11 Mg^{2+}, 12 Cu^{2+}, 13 Fe^{2+}, 14 Fe^{3+}.

meant that, neither hydrogen bond nor polarity from protic/aprotic solvent could induce a ring-opening reaction of spirolactam in Rh-APD except H^+.

3.3. pH response

To illuminate the pKa modulation by hydrogen bond, pH titrations of Rh-APD, Rh-EA, Rh-AP and Rh-APDA in aqueous solutions were performed, shown in Fig. 3. The color and fluorescence of Rh-APD did not be observed in the pH ranges from 7.0 to 12, owing to its stable spirolactam. When pH value was adjusted from 7.0 to 5.5, the fluorescent intensity at 585 nm increased gradually. Meanwhile, the absorption intensity at 560 nm increased in two folds. The enhanced emission and absorption meant that there was a ring-opening reaction of spirolactam induced by H^+. Rh-EA, Rh-AP and Rh-APDA showed similar changes for absorption and emission in the process of acidification. The pKa values of Rh-EA, Rh-AP and Rh-APDA were 3.21 (±0.09), 4.51 (±0.14) and 4.66 (±0.08), respectively, calculated by fluorescent titration (Fig. 3a). Comparing Rh-EA with Rh-APD, it can be found that the steric hindrance can effectively tune pKa from 3.21 to 4.51. To further magnify steric hindrance, the pKa of Rh-APDA esterified from Rh-APD was 4.66, tightly clustering about nearly 4.51 (Rh-AP). There was a similar steric hindrance between Rh-AP and Rh-APD. But the pKa value of Rh-APD was up to 5.77 (±0.02), larger 1.2 pH units than that of Rh-AP. Similar results of pKa values between Rh-APD and Rh-AP could be also achieved from the fitting data of absorption titration (Fig. 3b). The enhancement on pKa of Rh-APD should be attributed to the assistance of moderate intramolecular hydrogen bond of O1–H1•••O3 (Fig. 1), which would play a vital role in tuning pKa value of rhodamine alkylamides. In addition, the sensitive pH range of Rh-APD (5.0–7.0) covered well with lysosomal pH (4.5–6.0) of living cells, which suggested that Rh-APD might be eminently suitable for lysosomal pH monitoring.

3.4. Selectivity of Rh-APD to metal ions

Excluding hydrogen ion, whether was there any other analytes that can induce the ring-opening reaction of spirolactam in Rh-APD? As known to all, metal ion was the main factor to regulate the ring switch of rhodamine spirolactam, which was used to design many fluorescent probe for various metal ions[37,38]. In order to verify the interference from metal ions, the selectivity of Rh-APD to various metal ions was investigated. 10.0 equiv. metal ions such as Na^+, K^+, Mg^{2+}, Ca^{2+}, Al^{3+}, Hg^{2+}, Cr^{3+}, Mn^{2+}, Cd^{2+}, Zn^{2+},Cu^{2+}, Fe^{2+} and Fe^{3+} were added into Rh-APD aqueous solution (2×10^{-5} M) at pH 7.4, respectively. As illustrated in Fig. 4, there were not apparent changes for absorption intensity at 560 nm and emission intensity at 585 nm, upon addition of various metal ions.

3.5. Reversibility of the response of Rh-APD to H^+

The reversible response of Rh-APD to pH between 4.5 and 7.0 was illuminated in Fig. 5. Adjusted the pH value of aqueous solution (C_2H_5OH: H_2O, 1/1, v/v) to ~4.5, a pink color of solution could be instantly captured by naked-eyes, and in the meanwhile a red emission at 585 nm was detected upon excitation at 365 nm. Whereas the pH value was adjusted to ~7.0, both the color and fluorescence of Rh-APD faded fast. Rh-APD possessed an excellent reversibility towards pH, suggested that Rh-APD might be a potential indicator for pH monitoring in the environmental water system.

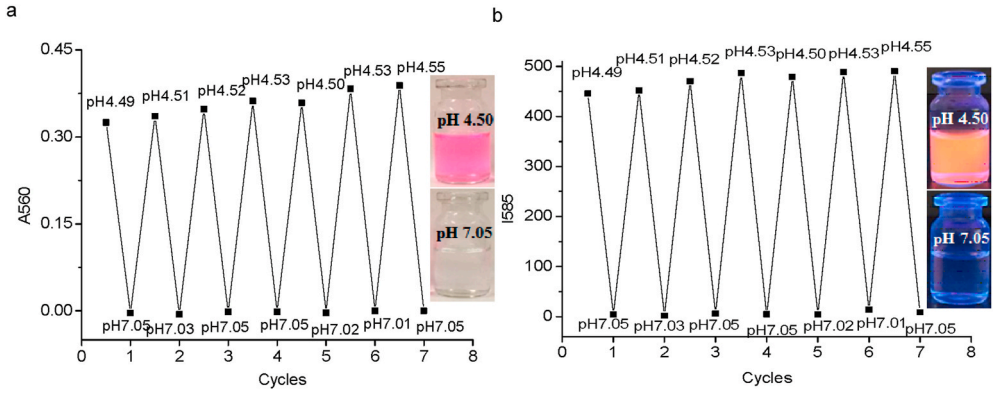

Fig. 5. Absorption intensity at 560 nm (a) and fluorescent intensity at 585 nm (b) of Rh-APD (2×10^{-5} M) in C_2H_5OH: H_2O (1/1, v/v) solution at pH 4.5 and 7.0. Inset: absorption and emission color of Rh-APD in aqueous solution at pH 4.5 and 7.0, respectively.

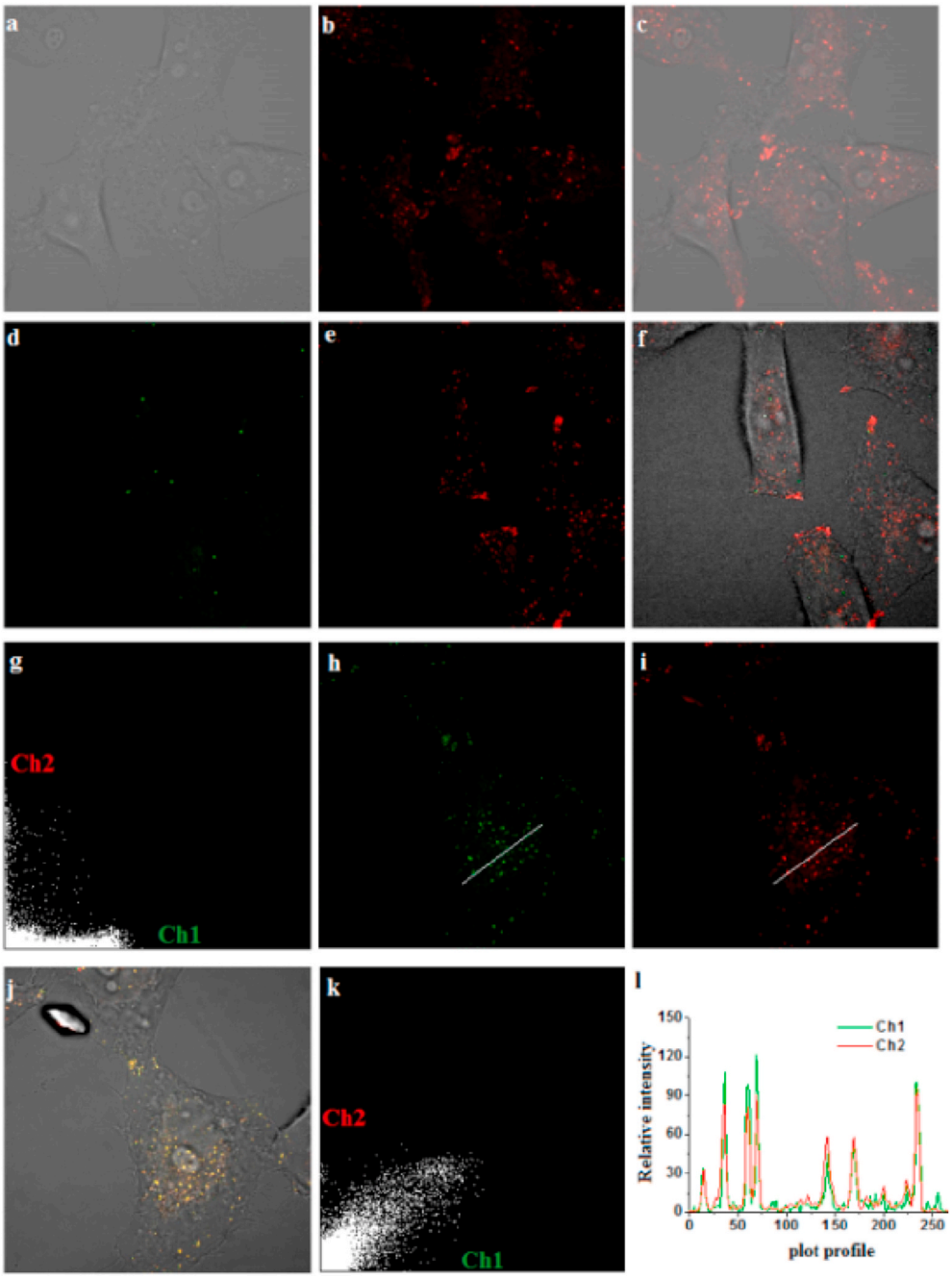

Fig. 6. The fluorescent imaging of MCF-7 cells stained with Rh-APD: (a) Differential interference contrast channel (DIC) (b) Red Channel (Ex: 559 nm, Em: 575–665 nm) (c) Merged image of DIC and Red Channel, (d–g) the fluorescent imaging of MCF-7 cells stained withBODIPY®493/503 and Rh-APD: (d) Green Channel Ch1: λex 488 nm, λem 500–520 nm, (e) Red Channel Ch2: λex 559 nm, λem 575–655 nm, (f) Merged image, (g) Intensity correlation plot of Ch1 and Ch2, (h–l) The fluorescent imaging of MCF-7 cells stained with Lyso-tracker DND-26 and Rh-APD (h) Green Channel Ch1:λex 488 nm, λem 500–520 nm (i) Red Channel Ch2: λex 559 nm, λem 575–655 nm, (j) Merged image (k) Intensity correlation plot of Ch1 and Ch2, (l) Intensity profile of region of interest (ROI, white line) cross MCF-7 cells.

3.6. Bioimaging

For the sensitive spectral responses of Rh-APD at pH range from 5.0 to 7.0, Rh-APD was expected to be used as a powerful tool for fluorescent imaging of cells' acidic environment. As shown in Fig. 6, MCF-7 cells stained with Rh-APD can glow with red discrete fluorescence in subcellular locations, upon excitation at 559 nm (Fig. 6a–c). Furthermore, large red discrete regions distributed in the cytoplasm near the cell periphery, suggested that Rh-APD might be targetable for lipid droplet or lysosome. Herein, lipid droplet tracker BODIPY®493/503 and Lyso-tracker DND-26 were chosen for co-localization imaging with Rh-APD, respectively (Fig. 6d–l). MCF-7 cells stained with BODIPY®493/503 showed the dotted fluorescence, which did not coincide with fluorescence of Rh-APD in merged imaging (Fig. 6d–f). Intensity correlation plot of Ch1 and Ch2 in Fig. 6g provided further evidence that Rh-APD can't specifically enrich into lopid droplet. The Pearson's coefficient and Mander's overlap coefficient were 0.23 and 0.21, respectively. Finally, the co-localization imaging of Rh-APD and lyso-tracker DND-26 were illustrated in Fig. 6h–l. Observed with the optical microscope, MCF-7 cells stained with DND-26 and Rh-APD emitted green and red fluorescence, respectively. There was a good overlay between DIC image, DND-26 and Rh-APD within the cells (Fig. 6j). Intensity correlation plot of DND-26 and Rh-APD distributed typically on the diagonal (Fig. 6k). Moreover, the Pearson's coefficient and Mander's overlap coefficient were high up to 0.94 and 0.96. Intensity profile of linear ROI across MCF-7 cells stained with DND-26 and Rh-APD also varied in close synchrony. These results indicated that Rh-APD can specifically accumulate in lysosomes of MCF-7 cells. Different from amino-containing targetable groups, the hydroxyl group of amino-1,3-propanediol in Rh-APD could induce rhodamine spirolactam into lysosome while avoiding the "alkalizing effect".

To evaluate the ability of Rh-APD for pH fluctuation monitoring in

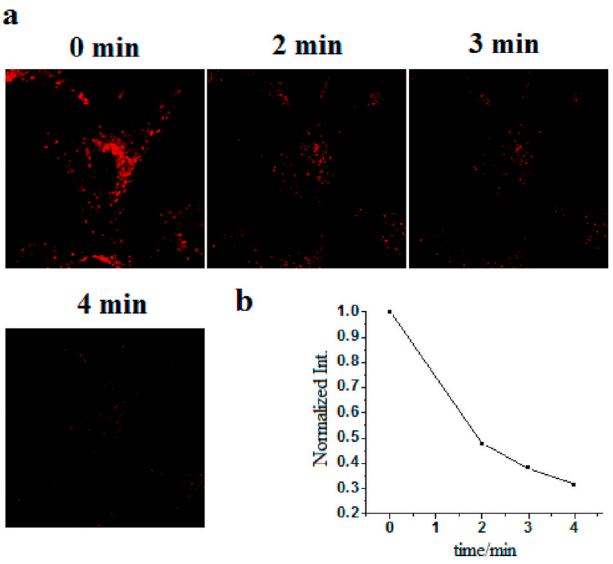

Fig. 7. Time course of fluorescence imaging (a) and fluorescent intensity (b) of MCF-7 cells stained with Rh-APD (5 μM), upon addition of choroquine (50 μM).

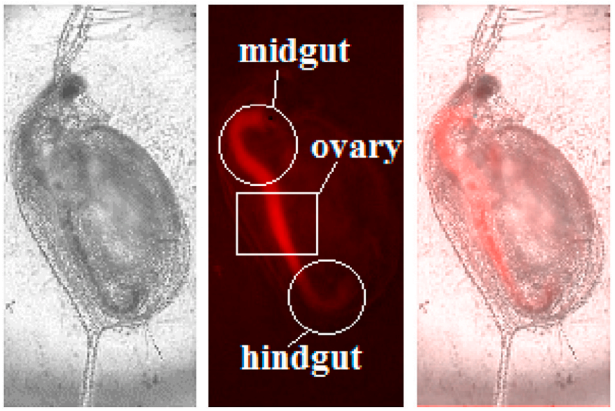

Fig. 8. Fluorescent imaging of Daphnia magna stained with Rh-APD (5 μM).

lysosomes, the time course of fluorescent imaging of MCF-7 cells stimulated by choroquine and Daphnia magna imaging were demonstrated in Fig. 7. After choroquine was added into MCF-7 cells stained with Rh-APD, the fluorescent intensity decreased along with the prolongation of the time. Two minutes later the average fluorescent intensity of MCF-7 image decreased by more than half from 100% to 47% (Fig. 7b). The red fluorescence of MCF-7 cells fade away with prolonging the contact time. After 4 min, the average fluorescent intensity of MCF-7 cells reduced up to 70%. Significantly, as a result of Rh-APD intake, red fluorescence was visible in the digestive tract and ovary of Daphnia magna (Fig. 8)[39]. The fluorescence at midgut was fainter than that at the hindgut, which indicated that the pH value at the midgut was more acidic. Different from the midgut and hindgut of Daphnia magna, the fluorescence of the ovary was very bright, suggesting the strong acidity at the ovary of Daphnia magna. These results revealed that Rh-APD would be a potential indicator for pH fluctuation in lysosomes of MCF-7 cells and the gut of Daphnia magna.

4. Conclusion

In summary, a series of rhodamine spirolactams such as Rh-APD, Rh-EA, Rh-AP, Rh-APDA, bearing flexible alkyl chains were developed to verify the pKa tuning by hydrogen bond. Rh-AP and Rh-APDA had similar pKa values, 4.51 (±0.14) and 4.66 (±0.08), which was larger than that of Rh-EA (3.21 ± 0.09). Different from rhodamine spirolactam Rh-AP and Rh-APDA, the pKa of Rh-APD was large up to 5.7 (±0.02), owing to its intramolecular hydrogen bond derived from hydroxyl of amino-1,3-propanediol between carbonyl of spirolactam. Gaussian stimulation demonstrated a moderate intramolecular hydrogen bond in Rh-APD at DFT/B3LYP/6–31 G(d) level. Neither in protic solvent nor aprotic solvent Rh-APD maintained closed form, and the spirolactam couldn't be induced open-state by metal ions. Cell imaging showed that Rh-APD could specifically accumulate in lysosomes and evaluate the pH fluctuation of lysosomes in live MCF-7 cells. Finally, Rh-APD also was used to indicate the acidity of gut and ovary of Daphnia magna. We expect that Rh-APD would be a promising fluorescent probe for pH indication in lysosomes of living cells and water fleas.

Credit author statement

Lei Min: Compound synthesis, Geometry Optimization, Writing-Original draft preparation.
Xintong Li: Compound synthesis, Analytical Measurements.
Weiliang Zhang: Compound synthesis, Data curation.
Xinfu Zhang: Data curation, Bio-imaging.
Ying Zhang: Supervision, Validation.
Haibo Yu: Conceptualization, Methodology, Writing-Reviewing and Editing, Funding acquisition.
Yi Xiao: Writing-Reviewing and Editing.

CRediT authorship contribution statement

Lei Min: Compound synthesis, Geometry Optimization, Writing - original draft, preparation. **Xintong Li:** Compound synthesis, Analytical Measurements. **Weiliang Zhang:** Compound synthesis, Data curation. **Xinfu Zhang:** Data curation, Bio-imaging. **Ying Zhang:** Supervision, Validation. **Haibo Yu:** Conceptualization, Methodology, Writing - review & editing, Funding acquisition. **Yi Xiao:** Writing - review & editing.

Declaration of competing interest

The authors declare that they have no known competing financial interests or personal relationships that could have appeared to influence the work reported in this paper.

Acknowledgment

This work was supported by the grants from Liaoning Revitalization Talents Program (XLYC1907002), Program of Liaoning Province Education Administration (LJC201913), Shenyang Young and Middle-aged Innovators Program (RC200569), Open Research Fund from State Key Laboratory of Fine Chemicals (KF1906), Joint Research Fund Liaoning-Shenyang National Laboratory for Materials Science (20180510044), Innovative Team Project of Education Department of Liaoning Province (LT2018018) of China, the Key Laboratory Project of Shenyang Municipal Science and Technology Plan (19-109-1-003) of China and Liaoning University Students' Innovation and Entrepreneurship Training Program (D202011282108594689). Special thanks to Dan Wang for providing the comparison analogs.

Appendix A. Supplementary data

Supplementary data to this article can be found online at https://doi.org/10.1016/j.dyepig.2021.109173.

References

[1] Chen X, Pradhan T, Wang F, Kim JS, Yoon J. Chemosensors based on spiroring-opening of xanthenes and related derivatives. Chem Rev 2012;112:1910–56.
[2] Beija M, Afonso CAM, Martinho JMG. Synthesis and applications of Rhodamine derivatives as fluorescent probes. Chem Soc Rev 2009;38:2410–33.

[3] Xu X, Chen S, Wu Q. Surface molecular imprinting on polypropylene fibers for rhodamine B selective adsorption. J Colloid Interface Sci 2012;385:193–201.
[4] Escobar CD, dos Santos JHZ. Effert of the sol-gel on the textural characteristics of silicaimprinted with Rhodamine B. J Separ Sci 2014;37:868–75.
[5] Rosenthal Peretz P. Thermochromic and hyperchromic effects in rhodamine B solutions. J Phys C 1979;83:351.
[6] Shankar BV, Patnaik A. A new pH and thermo-responsive chiral hydrogel for stimulated release. J Phys Chem B 2007;111:9294–300.
[7] Tomaselli S, Giovanella U, Pagano K, Leone G, Zanzoni S, Assfalg M, et al. Encapsulation of a rhodamine dye within a bile acid binding protein:toward water processable functional bio host-guest materials. Biomacromolecules 2013;14:3549–56.
[8] Barranco A, Groening P. Fluorescent plasma nanocomposite thin films containing nonaggregated rhodamine 6G laser dye molecules. Langmuir 2006;22:6719–22.
[9] Folling J, Belov V, Kunetsky R, Medda R, Schonle A, Egner A, et al. Photochromic rhodamines provide nanoscopy with optical sectioning. Angew Chem Int Ed 2007;46:6266–70.
[10] Qi Q, Chi W, Li Y, Qiao Q, Chen J, Miao L, Zhang Y, Li J, Ji W, Xu T, Liu X, Yoon J, Xu Z. A H-bond strategy to develop acid-resistant photoswitchable rhodamine spirolactams for super-resolution single-molecule localization microscopy. Chem Sci 2019;10:4914–22.
[11] Yuan X, Zhang T, Yan J, Chen X, Wang L, Liu X, Zheng K, Zhang N. A simple acidic 'turn-on' fluorescent pH probe based on BOPYIN and its visual detection and cellular imaging. Dyes Pigments 2020;177. 108318-8.
[12] Jin D, Wang B, Hou Y, Du Y, Li X, Chen L. Novel near-infrared pH-sensitive cyanine-based fluorescent probes for intracellular pH monitoring. Dyes Pigments 2019;170:107612–7.
[13] Chen G, Fu Q, Yu F, Ren R, Li Y. Wide-acidity-range pH fluorescence probes for evaluation of acidification in mitochondria and digestive tract mucosa. Anal Chem 2017;89:8509–16.
[14] Tan J-L, Yang T-T, Liu Y, Zhang X, Cheng S-J, Zuo H, et al. Sensitive detection of strong acidic condition by a novel rhodamine-based fluorescent pH chemosensor. Luminescence 2016;31:865–70.
[15] Yu K-K, Li K, Hou J-T, Qin H-H, Xie Y-M, Qian C-H, et al. Rhodamine-based lysosome-targeted fluorescence probes: high pH sensitivity and their imaging application in living cells. RSC Adv 2014;4:33975–80.
[16] Zhang W-S, Tang B, Liu X, Liu Y-Y, Xu K-H, Ma J-P, et al. A highly sensitive acidic pH fluorescent probe and its application to HepG2 cells. Analyst 2009;134:367–71.
[17] Georgiev NI, Bryaskova R, Tzoneva R, Ugrinova I, Detrembleur C, Miloshev S, et al. A novel pH sensitive water soluble fluorescent nanomicellar sensor for potential biomedical applications. Bioorg Med Chem 2013;21:6292–302.
[18] Li B, Ge G-B, Wen L-L, Yuan Y, Zhang R, Peng X-J, et al. A lysosomal probe for monitoring of pH in living cells and ovarian tumour. Dyes Pigments 2017;139:318–25.
[19] Lv H-S, Liu J, Zhao J, Zhao B-X, Miao J-Y. Highly selective and sensitive pH-responsive fluorescent probe in living Hela and HUVEC cells. Sensor Actuator B Chem 2013;177:956–63.
[20] Yu K-K, Hou J-T, Li K, Yao Q, Yang J, Wu M-Y, et al. A single design strategy for dual sensitive pH probe with a suitable range to map pH in living cells. Sci Rep 2015;5(1–11):15540.
[21] Lee MH, Han J-H, Lee JH, Park N, Kumar R, Kang C, et al. Two-color probe to monitor a wide range of pH values in cells. Angew Chem Int Ed 2013;52:6206–9.
[22] Xue Z-W, Zhao H, Liu J, Han J-H, Han S-F. Imaging lysosomal pH alteration in stressed cells with a sensitive ratiometric fluorescence sensor. ACS Sens 2017;2:436–42.
[23] Hu Z-Q, Li M, Liu M-D, Zhuang W-M, Li G-K. A highly sensitive fluorescent acidic pH probe based on rhodamine B diethyl-2-aminobutenedioate conjugate and its application in living cells. Dyes Pigments 2013;96:71–5.
[24] Lv H-S, Huang S-Y, Zhao B-X, Miao J-Y. A new rhodamine B-based lysosomal pH fluorescent indicator. Anal Chim Acta 2013;788:177–82.
[25] Yuan L, Lin W-Y, Feng Y-M. A rational approach to tuning the pKa values of rhodamines for living cell fluorescence imaging. Org Biomol Chem 2011;9:1723–6.
[26] Czaplyski WL, Purnell GE, Roberts CA, Allred RM, Harbron EJ. Substituent effects on the turn-on kinetics of rhodamine-based fluorescent pH probes. Org Biomol Chem 2014;12:526–33.
[27] Lee D, Swamy KMK, Hong J, Lee S, Yoon J. A rhodamine-based fluorescent probe for the detection of lysosomal pH changes in living cells. Sensor Actuator B Chem 2018;266:416–21.
[28] Ye Z-W, Yu H-B, Yang W, Zheng Y, Li N, Bian H, et al. Strategy to lengthen the on-time of photochromic rhodamine spirolactam for super-resolution photoactivated localization microscopy. J Am Chem Soc 2019;141:6527–36.
[29] Song Y, Zheng Y, Zhang S, Song Y-X, Niu M-D, Li Y-H, et al. Always-on and water-soluble rhodamine amide designed by positive charge effect and application in mitochondrion-targetable imaging of living cells. Sensor Actuator B Chem 2019;286:32–8.
[30] Yu H-B, Li G-L, Zhang B, Zhang X-F, Xiao Y, Wang J-Q, et al. A neutral pH probe of rhodamine derivatives inspired by effect of hydrogen bond on pKa and its organelle-targetable fluorescent imaging. Dyes Pigments 2016;133:93–9.
[31] Zhao X-X, Ge D, Dai X, Wu W-L, Miao J-Y, Zhao B-X. A water-soluble pH fluorescence probe based on quaternary ammonium salt for bioanalytical applications. Spectrochim Acta 2015;151:218–24.
[32] Devi M, Dhir A, Pradeep CP. A tris(hydroxymethyl)aminomethane-rhodamine spirolactam derivative as dual channel pH and water sensor and its application to bio imaging. Eur J Org Chem 2015;21:4650–7.
[33] Xia Y, Liu X-Y, Wang D, Wang Z-C, Liu Q, Yu H-B, et al. A fluorometric and mitochondrion-targetable probe for rapid, naked-eye test of hypochlorite in real samples. Chin Chem Lett 2018;29:1517–20.
[34] Wang D, Wang Z-C, Li Y-H, Song Y, Song Y-T, Zhang M-Y, et al. A single rhodamine spirolactam probe for localization and pH monitoring of mitochondrion/lysosome in living cells. New J Chem 2018;42:11102–8.
[35] Wang Z-C, Zhang Q-H, Liu J-W, Sui R, Li Y-H, Li Y, et al. A twist six-membered rhodamine-based fluorescent probe for hypochlorite detection in water and lysosomes of living cells. Anal Chim Acta 2019;1082:116–25.
[36] Jeffrey GA. An introduction to hydrogen bond. New York: Oxford University; 1997.
[37] Dujols V, Ford F, Czarnik AW. A long-wavelength fluorescent chemodosimeter selective for Cu(II) ion in water. J Am Chem Soc 1997;119:7386–7.
[38] Kim HN, Lee MH, Kim HJ, Kim JS, Yoon J. A new trend in rhodamine-based chemosensors: application of spirolactam ring-opening to sensing ions. Chem Soc Rev 2008;37:1465–72.
[39] Chiang SC, Du NS. Fauna sinica-Crustacea, freshwater cladocera. Peking. Science Press; 1979.